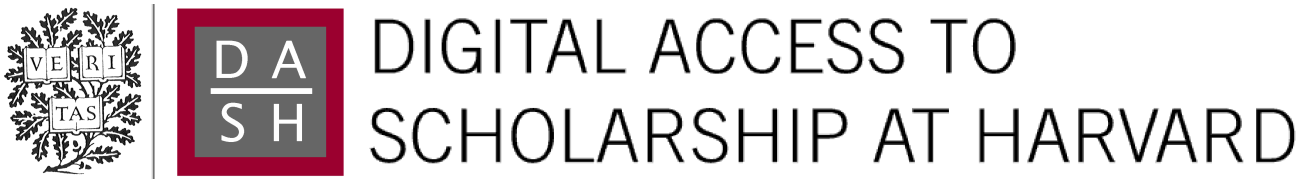

Notch Inhibition Allows Oncogene-Independent Generation of iPS Cells

Notch inhibition allows oncogene independent generation of iPS cells

Justin K. Ichida[1,2,9]*, Julia TCW[1,2,3]*, Luis A. Williams[1,2], Ava C. Carter[1, 2], Yingxiao Shi[9], Marcelo T. Moura[1,2], Michael Ziller[1,4],Sean Singh[1,2], Giovanni Amabile[5],Christoph Bock[1,4], Akihiro Umezawa[6], Lee L. Rubin[1], James E. Bradner[7,8], Hidenori Akutsu[6], Alexander Meissner[1,4], Kevin Eggan[1,2,3]

[1] Harvard Stem Cell Institute, Department of Stem Cell and Regenerative Biology, Harvard University, Cambridge, MA 02138, USA

[2] Howard Hughes Medical Institute and Stanley Center for Psychiatric Research

[3] Department of Molecular and Cellular Biology, Harvard University, Cambridge, MA 02138, USA

[4] Broad Institute of MIT and Harvard, 7 Cambridge Center, Cambridge, Massachusetts 02142, USA

[5] Harvard Stem Cell Institute, Harvard Medical School, Boston, MA

[6] Department of Reproductive Biology, National Research Institute for Child Health and Development, 2-10-1 Okura, Setagaya, Tokyo 157-8535, USA

[7] Department of Medical Oncology, Dana-Farber Cancer Institute, 450 Brookline Avenue, Boston, MA 02215, USA

[8] Department of Medicine, Harvard Medical School, 25 Shattuck Street, Boston, MA 02115, USA

[9] Department of Stem Cell Biology and Regenerative Medicine, University of Southern California, 1425 San Pablo Street, Los Angeles, CA 90033, USA

* These authors contributed equally to this work.

Abstract

The reprogramming of somatic cells to pluripotency using defined transcription factors holds great promise for biomedicine. However, human reprogramming remains inefficient and relies either on the use of the potentially dangerous oncogenes KLF4 and CMYC or the genetic inhibition of the tumor suppressor gene p53. We hypothesized that inhibition of signal transduction pathways that promote differentiation of the target somatic cells during development might relieve the requirement for non-core pluripotency factors during iPSC reprogramming. Here, we show that inhibition of Notch significantly improves the efficiency of iPSC generation from mouse and human keratinocytes by suppressing p21 in a* p53*-independent manner and thereby enriching for undifferentiated cells capable of long-term self-renewal. Pharmacological inhibition of Notch enabled routine production of human iPSCs without KLF4 and CMYC while leaving* p53 *activity intact. Thus, restricting the development of somatic cells by altering intercellular communication enables the production of safer human iPSCs.

Use of the potent oncogenes *KLF4* and *CMYC* in the generation of induced pluripotent stem cells (iPSCs) limits their translational utility [1,2]. Currently, elimination of these genes during human iPSC reprogramming requires suppression of p53 activity [2-16], which in turn results in the accumulation of genetic mutations in the resulting iPSCs [8]. Therefore, there remains a real need for reprogramming approaches that enable iPSC generation without the use of *KLF4* and *CMYC* while leaving p53 activity intact.

In part to address this need, several groups have undertaken chemical screens to identify small molecules that can improve reprogramming [17-21]. Thus far, the majority of active compounds are thought to improve reprogramming by inhibiting chromatin-modifying enzymes or by reinforcing the transcriptional network associated with the pluripotent state [17-22]. Consistent with their proposed mechanisms of action, these chemicals generally function in cellular intermediates that arise late in reprogramming, catalyzing their final conversion into iPSCs [19,22]. It is currently unclear whether known chemicals are sufficient for generating iPSCs from adult human cells, which are consistently more difficult to reprogram than mouse embryonic fibroblasts [23].

Given the likely need for additional reprogramming chemicals and the knowledge that most known compounds act late in this process, we reasoned it would be valuable to identify small molecules that improve reprogramming by acting early, perhaps within the somatic cells themselves. We reasoned that one approach towards this goal would be to identify chemicals that could modulate signal transduction cascades in somatic cell populations to enrich for those cells with an enhanced capacity for reprogramming. We reasoned that if such compounds could be identified, they might expand the translational utility of chemical reprogramming.

It has been recognized that the extent of a target cell's differentiation is an important determinant of the efficiency by which it can be reprogrammed [24-26]. We therefore hypothesized that chemically driving somatic cells into a more potent "stem cell" state might improve their reprogramming. To test this hypothesis, we chose to ask whether known chemical inhibitors of the Notch signaling pathway could aid in reprogramming.

The Notch signaling pathway is highly conserved and regulates the proliferation and differentiation of many distinct progenitor cell and stem cell types [27]. Notch ligands are generally transmembrane proteins that require contact between two cells in order to mediate signal transduction [28]. In skin, Notch promotes differentiation by directly activating *p21* expression, which in turn blocks proliferation and induces the differentiation of keratinocyte stem cell populations [29,30]. We therefore hypothesized that inhibition of Notch in keratinocytes might enhance iPSC generation by inhibiting differentiation and enriching more easily reprogrammed progenitor cells. We also felt that keratinocytes were an attractive model for testing our hypothesis because if Notch inhibition did have an effect, it could be immediately translated to the production of patient-specific iPSCs [31,32].

Here, we show that Notch inhibition significantly improves the efficiency of iPSC generation from mouse and human keratinocytes by suppressing p21 and thereby enriching undifferentiated cells with increased reprogramming potential. In addition, pharmacological inhibition of Notch enabled the efficient production of human iPSCs without *KLF4* and *CMYC* while leaving p53 activity intact, resulting in the production of safer human iPSCs.

Results

DAPT treatment promotes keratinocyte reprogramming

Notch signaling is activated by the γ-secretase complex, which cleaves the membrane-tethered Notch receptor upon ligand binding and generates a free intracellular domain that can translocate to the nucleus and modulate transcription [27]. It has previously been shown that the γ-secretase inhibitor DAPT (Fig. 1a) can block Notch signaling in mouse keratinocytes [33]. As expected, 10 μM DAPT treatment of both neonatal mouse and human keratinocytes transduced with the iPSC reprogramming factors increased abundance of the full-length Notch receptor, reduced levels of cleaved Notch intracellular domain (NICD) (Supplementary Results, Supplementary Fig. 1a), and decreased expression of the Notch-target genes *Hey1*, *Hes1*, *Hes5*, and *Col6a1* (Supplementary Fig. 1b**)**.

To determine whether inhibition of Notch could increase the efficiency of reprogramming, we transduced *Oct4*::GFP mouse or human keratinocytes with *Oct4*, *Sox2*, *Klf4*, and *cMyc* and cultured the resulting cells for 25 days either in the presence or absence of DAPT. We found that the addition of 10 μM DAPT led to a significant, 4-fold increase in the number of resulting *Oct4::*GFP+ mouse and NANOG+/TRA-1-81+ human iPSC colonies (Fig. 1b).

We wondered whether this increase in reprogramming activity might allow the generation of iPSCs from keratinocytes without *Klf4* and *cMyc*. Indeed, although transduction of *Oct4* and *Sox2* alone were not sufficient to induce keratinocyte reprogramming, *Oct4* and *Sox2* combined with DAPT treatment routinely yielded mouse

and human iPSC colonies (Figs. 1c,d and Supplementary Fig. 2a). This effect was specific to *Oct4* and *Sox2*-transduced cells because other 2-factor combinations did not yield iPSCs in the presence of DAPT (Fig. 1c).

To determine whether these putative iPS cell lines were pluripotent, we subjected them to a "scorecard" assay for pluripotency that we recently developed [34]. We found that these cell lines were indeed composed of pluripotent cells and that they performed comparably to human embryonic stem cells (ESCs) in their expression of pluripotency-associated genes and differentiation propensities (Supplementary Figs 2b, c). To further confirm their differentiation capacity, we also injected the *OCT4*, *SOX2* + DAPT human cells into immunocompromised mice and found that they readily formed teratomas containing differentiated cells (Fig. 1e). Moreover, when injected into blastocysts, the *Oct4, Sox2* + DAPT mouse cells contributed to the development of chimeric mice (Supplementary Fig. 2d), including the germ-line (Supplementary Fig. 2e).

Many applications of iPS cells would require the DAPT-dependent generation of *KLF4* and *CMYC*-free iPSCs from adult keratinocytes. Therefore, we determined if DAPT treatment increased the reprogramming potential of adult human keratinocytes. As with mouse and human neonatal keratinocytes, we found that DAPT treatment of *KLF4*, *SOX2*, *OCT4*, and *CMYC*-transduced adult human keratinocytes significantly improved their rate of reprogramming (Supplementary Fig. 2f) and also enabled the generation of iPSCs with just *OCT4* and *SOX2* (Fig. 1f, Supplementary Fig. 2g). The scorecard assay again verified that these 2-factor iPSCs were pluripotent (Supplementary Figs 2b, c). Together, these results demonstrate that DAPT reliably enables the generation of *bona fide* mouse and human iPSCs from keratinocytes without *KLF4* and *CMYC*.

Notch inhibition promotes reprogramming

Our results thus far suggest that antagonizing Notch signaling in keratinocytes may promote their conversion into iPSCs. To begin verifying that NOTCH was indeed the functional target of DAPT during reprogramming, we tested a structurally distinct γ-secretase inhibitor, DBZ [35](Fig. 2a), for activity in iPSC generation. When we treated human keratinocytes with DBZ, we observed significant reductions in the levels of the intracellular domain of the NOTCH receptor (Supplementary Fig.1a) and the NOTCH-dependent genes *HES1* and *HES5* (Supplementary Fig. 3a), indicating that DBZ administration inhibited NOTCH signaling. Consistent with the notion that NOTCH inhibition increases the rate of reprogramming, DBZ significantly stimulated the formation of human iPSC colonies (Fig. 2b).

Both DBZ and DAPT could have effects on the processing of unidentified γ-secretase substrates that are distinct from NOTCH, which might also impact reprogramming efficiency. If the beneficial effects of DAPT on reprogramming were being mediated through the specific inhibition of NOTCH signaling rather than through some other target of γ-secretase, then we reasoned that constitutive activation of NOTCH signaling should eliminate the beneficial effect of DAPT. Consistent with this notion, we found that overexpression of the NOTCH intracellular domain (Supplementary Fig. 3b) stimulated the expression of NOTCH-target genes (Supplementary Fig. 3c) and completely blocked the positive effects of DAPT on reprogramming (Fig. 2c). Conversely, we reasoned that antagonizing the transcriptional activity of NOTCH should increase the rate of keratinocyte reprogramming. Indeed, when we suppressed NOTCH activity by overexpressing a dominant-negative form of *MAML1* (Fig. 2d), a

transcriptional co-activator for NOTCH [36,37], we observed an increase in iPSC generation from keratinocytes transduced with all 4 reprogramming factors (Fig. 2e). Therefore, we conclude that the inhibition of NOTCH signaling promotes the reprogramming of both human and mouse keratinocytes.

In order to understand how Notch inhibition promotes iPSC generation, we first determined when in the reprogramming process it was required. We treated mouse keratinocytes with DAPT either before or both before and after transduction with reprogramming factors. While treatment both before and after transduction yielded a 4-fold increase in iPSC generation, we found that pre-treatment alone resulted in a significant 2.5-fold enhancement in reprogramming efficiency (Supplementary Fig. 4a). To more precisely pinpoint the effective post-transduction treatment window, we transduced human keratinocytes with *KLF4*, *OCT4*, *SOX2*, and *CMYC* and administered DAPT or DBZ from days 1-6, 6-11, 11-16, or 1-16 after viral infection (Figs 3a-c). Chemical inhibition of NOTCH signaling was most effective during early time points, significantly increasing iPSC generation when used from days 1-6 and 6-11 (Figs 3b, c). In contrast, a later treatment from days 11-16 had little effect on reprogramming (Figs 3b, c). Together, these results indicate that Notch inhibition can act on the starting keratinocytes and at early time points just after the initiation of transcription factor overexpression to enhance reprogramming.

Notch inhibition acts by suppressing p21 expression

One way that Notch inhibition could promote iPSC formation is by activating the expression of the reprogramming transcription factors from their endogenous loci.

However, when we treated human keratinocytes with DAPT and analyzed their gene expression, we found that levels of *KLF4*, *OCT4*, and *CMYC* actually decreased and *SOX2* did not significantly change (Supplementary Fig. 4b).

In the mammalian epidermis, Notch signaling functions as a switch that directly activates *p21* transcription, which in turn forces keratinocytes to exit the cell cycle and begin differentiating [38]. To determine if chemical inhibition of Notch signaling in keratinocytes might be enhancing their reprogramming potential by suppressing *p21*, we measured p21 levels in human keratinocytes in the presence and absence of DAPT. Consistent with previous reports [38], we found that Notch inhibition decreased the levels of *p21* mRNA and protein in these cells (Supplementary Fig. 4c, Fig. 3d). In addition, DAPT treatment slightly decreased the level of FLAG-tagged p21 protein expressed by an exogenous retrovirus, indicating that Notch may also regulate p21 post-transcriptionally (Supplementary Figs. 4d, e). Consistent with these observations, Notch inhibition suppressed expression of *INVOLUCRIN*, which is expressed in more differentiated keratinocytes (Fig. 3e).

To verify that Notch inhibition promotes iPSC reprogramming by suppressing p21, we performed 2-factor (*Oct4* and *Sox2*) and 4-factor reprogramming in keratinocytes with p21 siRNA/shRNA in the presence or absence of DAPT. Mouse keratinocytes transduced with *Klf4, Sox2, Oct4*, and *cMyc* showed a similar increase in iPSC generation when treated with either 2.5 μm DAPT or p21 siRNA (Supplementary Fig. 4f). The efficiency of reprogramming with these two methods was not significantly different (Supplementary Fig. 4f), and treating with DAPT in the presence of the p21 siRNA did not produce a significant increase in iPSC formation (Supplementary Fig. 4f). Similarly,

suppression of p21 by shRNA (Supplementary Figs 4g, h) enabled the generation of iPSCs from human keratinocytes transduced with 2 or 4 factors at rates equivalent to DAPT treatment (Figs 3f, g). Again, supplementing p21 knockdown with DAPT treatment did not result in a significant increase in iPSC formation (Figs 3f, g). These results indicate that p21 suppression and DAPT have similar effects on iPSC generation from keratinocytes and that DAPT does not provide an additional advantage over p21 suppression alone.

If Notch inhibition and p21 suppression indeed blocks keratinocyte differentiation, the p21-treated keratinocytes would be predicted to display an increase in their long-term proliferative capacity [39]. The ability to form large colonies on collagen demonstrates the ability of keratinocytes to self-renew extensively and is a functional property unique to undifferentiated cells of this lineage [39]. In contrast, differentiated keratinocytes senesce after only a few rounds of division and do not form colonies [39]. DAPT treatment of human keratinocytes for 6 days significantly increased the number of cells capable of forming large colonies when cultured for an additional 14 days in the absence of the chemical (Supplementary Fig. 4i). The resulting 4-fold increase in colony formation rate was similar in magnitude to the elevation in iPSC generation with DAPT treatment (Fig. 1b). To determine if this increased self-renewal capacity was indeed promoting reprogramming, we transduced keratinocytes with p21 to limit their replication and attempted to reprogram them either with or without DAPT. The forced p21 expression severely impaired the self-renewal potential of the keratinocytes (Supplementary Fig. 4j) and inhibited iPSC formation after transduction with the 4 reprogramming factors and treatment with DAPT (Fig. 3h).

Because Notch inhibition does not promote fibroblast replication [40], if this is the mechanism by which DAPT improves reprogramming, we would not expect chemical treatment to affect mouse embryonic fibroblast [41] reprogramming [41]. Indeed, DAPT treatment of MEFs transduced with all 4 reprogramming factors did not affect the rate of iPSC generation (Supplementary Fig. 4k). Together, these results demonstrate that Notch inhibition promotes iPSC generation from keratinocytes by repressing their differentiation and enhancing their long-term replicative potential through p21 suppression.

Efficient reprogramming with Notch and DOT1L inhibition

Knowing that Notch inhibition enhances iPSC generation through this unique mechanism, we next wanted to compare its activity to previously described reprogramming molecules that act through other mechanisms [17,42-44] and identify any that DAPT might synergize with. When we transduced human neonatal keratinocytes with *KLF4*, *SOX2*, *OCT4*, and *CMYC* and treated them with various combinations of compounds shown to enhance reprogramming in other reports, including an activator of 3'-phosphoinositide-dependent kinase-1 (PDK1)[17], inhibitors of TGF-β, MEK, and GSK3β signaling [17], histone deacetylase inhibitors [17,42], histone methyltransferase inhibitors [17,44], and a DNA methyltransferase inhibitor [43], we found that DAPT treatment was the most potent at enhancing reprogramming (Fig. 4a). This remained true when we attempted reprogramming with only *OCT4* and *SOX2* (Fig. 4b).

However, an inhibitor of the histone methyltransferase DOT1L (iDOT1L) synergized *OCT4*, *SOX2* and DAPT to elevate the rate of iPSC generation by 10-fold

over the rate with *OCT4*, *SOX2* and DAPT alone, making it even more efficient than 4-factor reprogramming either with or without DAPT (Fig. 4b). The *OCT4* + *SOX2* + DAPT + iDOT1L colonies could be readily expanded and maintained NANOG and TRA-1-81 expression (Fig. 4c). These data indicate that Notch inhibition is a potent enhancer of reprogramming in keratinocytes that can synergize with chromatin-modifying compounds to induce pluripotency at a high efficiency with only *OCT4* and *SOX2*.

Notch inhibition does not compromise p53 activity

Previous studies of p53 and p21 in reprogramming have suggested that ectopic overexpression of reprogramming transcription factors can activate p53, which then induces either apoptosis or the expression of p21, thus inhibiting reprogramming [3,6]. Because suppression of the p53 pathway greatly facilitates iPSC generation, this approach has become an important part of reprogramming methods that reduce or eliminate integrating exogenous transcription factors [3,4]. However, because p53 inhibition allows the accumulation of genetic mutations during reprogramming [8], alternative approaches for increasing reprogramming efficiencies would be desirable. We therefore next asked whether Notch inhibition promotes reprogramming through a p53-dependent or independent pathway by analyzing the effects of DAPT and DBZ treatment on p53 and its target genes. First, we confirmed the finding that transduction with the iPSC reprogramming factors stimulated p53 activity (Fig. 5a). Chemical inhibition of Notch signaling in both human and mouse keratinocytes did not reduce the expression of p53 at the protein or mRNA level either before or after transduction with the reprogramming factors (Figs 5b,c and Supplementary Figs 5a, b). Moreover, transcriptional analysis of

DAPT-treated human and mouse keratinocytes revealed that the mRNA levels of the p53 target genes *Dr5*, *Puma,* and *Fas* were not decreased (Fig. 5c and Supplementary Figs 5a, b), supporting the notion that p53 activity was not suppressed by Notch inhibition.

To further confirm that DAPT treatment did not suppress p53 activity, we performed reprogramming experiments with and without DAPT after UV irradiation. UV exposure causes DNA damage, which in turn reduces reprogramming efficiencies by inducing p53-dependent apoptosis [8]. However, p53-deficient cells are resistant to the negative effects of UV irradiation on reprogramming [8]. Therefore, if p53 activity was maintained in DAPT-treated cultures, then we would expect a sharp decrease in reprogramming efficiency after UV irradiation. As a control for p53-deficiency, we performed 4-factor reprogramming with or without UV irradiation using keratinocytes in which we overexpressed a dominant-negative form of p53 (p53DD) [3] that suppressed p53 activity as evidenced by a decrease in the expression levels of p53-dependent target genes (Supplementary Fig. 5c). As expected, UV exposure did not impact the rate of iPSC generation when p53DD was expressed, functionally demonstrating that p53 activity was indeed impaired (Fig. 5d). In contrast, in the absence of p53DD overexpression, UV exposure sharply reduced the number of iPSCs generated in DMSO-treated cultures (Fig. 5d). Similarly, UV irradiation severely diminished the number of iPSC colonies in DAPT-treated cultures again suggesting that Notch inhibition does not suppress p53 activity during reprogramming (Fig. 5d).

Although the difference in reprogramming efficiency in p53-deficient versus DAPT-treated keratinocytes was clearly evident when UV irradiation was used to induce DNA damage, we next determined whether DNA damage was measurably influenced by

DAPT treatment under normal reprogramming conditions. To test this, we quantified phosphorylated histone H2AX (γH2AX) expression in 4-factor-transduced human keratinocytes treated with DAPT, p53DD, or p53 shRNA. Histone H2AX becomes phosphorylated in response to double strand DNA breaks, making it a reliable marker of DNA damage [8]. Pan-nuclear γH2AX expression results from replication-induced damage and could indicate insults sustained during reprogramming [8]. We found that 10 days after transduction, pan-nuclear γH2AX staining was significantly elevated in cultures treated with p53DD or p53 shRNA, which is consistent with a previous study in which elevated rates of DNA damage were observed in p53-deficient cells during reprogramming and in the resulting iPSCs [8] (Fig. 5e and Supplementary Figs 5d-f). The DAPT-treated cells, however, maintained low cell numbers with pan-nuclear γH2AX expression that were similar to the control cultures (Fig. 5e and Supplementary Fig. 5f). These results suggest that, in contrast to p53-deficiency, DAPT treatment did not promote the survival and reprogramming of cells with DNA damage.

To confirm that Notch inhibition does not prevent the apoptosis of compromised cells during reprogramming, we measured the fraction of TUNEL-positive nuclei in DAPT-treated cultures. Despite high rates of DNA damage in the p53-deficient reprogramming cultures, the percentage of TUNEL-positive nuclei was greatly reduced compared to a wild-type control, indicating that inactivation of p53 permitted the survival of cells with compromised genomes (Fig. 5f). In contrast, the percentage of TUNEL-positive cells was not significantly reduced by DAPT treatment (Fig. 5f).

In order to determine if DAPT enabled the efficient generation of iPSCs that displayed improved genomic integrity relative to their counterparts made through p53

suppression, we measured the copy number variation in iPSC lines made with DAPT or p53DD. Consistent with the γH2AX and TUNEL staining results, we found that iPSC lines derived in the presence of p53DD possessed an average of 4 indels/line, while iPSCs derived with a control GFP vector or 10 μm DAPT contained only 1 or .5 indels/line, respectively (Fig. 5g and Supplementary Fig. 6). Together, these experiments show that DNA damage is present during normal reprogramming conditions and that inhibition of p53 allows cells with damaged genomic material to persist. In contrast, Notch inhibition enhances reprogramming without compromising genomic integrity or promoting the survival of iPSCs that have undergone DNA damage.

Discussion

In summary, our findings suggest that signaling through the Notch pathway is a significant impediment to the early stages of the reprogramming of both mouse and human keratinocytes into iPSCs (Figure 6). Importantly, the mechanism by which Notch signaling likely inhibits reprogramming of mouse and human cells is by activating p21 independently of p53. Consistent with this hypothesis, treatment of reprogramming cultures with the γ-secretase inhibitors DAPT and DBZ reduced the levels of intracellular Notch and increased colony forming potential, leading to an increase in the rate of iPSC formation. Suppression of p21 expression by siRNA/shRNA was sufficient to replace Notch inhibition in reprogramming, and exogenous p21 blocked the beneficial effects of DAPT. Importantly, the resulting improvement in reprogramming activity did not come at the expense of a reduction in p53 activity or increased genomic instability (Figure 6).

Our findings have immediate and practical ramifications for the improved production of patient-specific human iPSCs. When taken together, our studies show that through pharmacological inhibition of NOTCH, it is routinely possible to produce human iPSCs with only *OCT4* and *SOX2*, rendering *CMYC* and *KLF4* dispensable and thereby reducing the oncogenic potential of the resulting cells. Furthermore, our findings enabled *CMYC* and *KLF4*-free iPSC production without inhibition of p53 or its target genes involved in apoptosis, allowing pro-apoptotic pathways that ensure genomic integrity to be engaged [8,10,11]. Thus, in this approach, the production of oncogene-free iPSC lines does not come at the expense of an increase in mutational load [8,10,11,45].

Studies using nuclear transplantation and defined transcription factors have shown that nuclei become less amenable to reprogramming as they advance developmentally [24-26]. Our study demonstrates that intercellular communication in somatic cultures can cause them to differentiate and lose their reprogramming potential, but that with small molecule treatment, it is possible to force them to remain in an undifferentiated, highly reprogrammable state. This approach synergized potently with chemical inactivation of the histone H3 methyltransferase DOT1L, allowing two-factor reprogramming at higher efficiency than with four transcription factors. This indicates that while histone methyltransferase inhibition had almost no effect on the reprogramming of differentiated keratinocytes, it had a profound ability to enhance the reprogramming of undifferentiated keratinocytes. Thus, somatic cells at different developmental stages respond differentially to chromatin-modifying signals during reprogramming. The combined chemical inhibition of NOTCH and DOT1L provides a new approach for boosting the

reprogramming potential of keratinocytes and is an attractive starting point for the identification of a small molecule reprogramming cocktail for human cells.

Acknowledgements
The authors would like to thank E. Son for assistance with microarray data analysis, S. Sato for assistance with chimera experiments, E. Kiskinis for assistance with nanostring analysis, and K. Koszka and M. Yamaki for assistance with teratoma experiments. The authors are grateful for the financial support that made this work possible. K.E. was supported by NIH R01 grant 5 R01 GM96067-03, NIH P01 grant GM099117 and HHMI. A.M was supported by NIH P01 grant GM099117. H.A. was supported by grants from the Ministry of Education, Culture, Sports, Science and Technology (MEXT) of Japan, Grant-in-aid for Scientific Research (21390456) and Grant-in-Aid for challenging Exploratory Research (22659304), and a grant from JST-CREST. J.K.I. was supported by a Stan and Fiona Druckenmiller/New York Stem Cell Foundation postdoctoral fellowship, NIH K99 grant 1K99NS077435-01A1, NIH R00 grant 4R00NS077435-03, and the Novartis Institutes for BioMedical Research. C.B. was supported by a Feodor Lynen Fellowship from the Alexander von Humboldt Foundation.

Author Contributions
A.M. and J.E.B. hypothesized Notch inhibition might aid reprogramming. J.K.I., J.T., A.M., A.U., L.L.R., and K.E. designed reprogramming and mechanistic experiments to test the hypothesis. J.K.I., J.T., A.C.C., L.A.W., Y.S., M.T.M., S.S., G.A., and H.A. performed reprogramming experiments and characterization of the iPSCs. C.B. and M.Z. performed bioinformatic analysis of transcriptional data characterizing the iPSCs. J.K.I., J. T., A.C.C., and Y.S. performed experiments to determine the mechanism of action of DAPT and Notch inhibition in reprogramming. K.E., J.K.I. and J.T. discovered and confirmed the mechanism of action of DAPT. K.E. and J.K.I. wrote the paper. All helped in paper revision.

Author Information
The authors declare no competing financial interests. Correspondence and requests for materials should be addressed to K.E. (keggan@scrb.harvard.edu), A.M. (alexander_meissner@harvard.edu), or H.A. (akutsu-h@ncchd.go.go.jp).

Figure 1. DAPT treatment promotes mouse and human keratinocyte reprogramming. a, Chemical structure of DAPT. **b,** The efficiency of iPSC generation from mouse and human keratinocytes transduced with *Oct4*, *Sox2*, *Klf4*, and *cMyc* with DMSO or DAPT treatment (DAPT used at 10 μM in mouse experiment). **c,** The efficiency of iPSC generation from mouse and human keratinocytes transduced with all combinations of 2 reprogramming factors with DMSO or 2.5 μM DAPT treatment from days 1-18 post-transduction. **d,** A P0 mouse and human iPSC colony generated using *OCT4*, *SOX2*, and DAPT, scale bars = 100 μm. **g,** Teratoma generated by iPSCs derived from human neonatal kerationcytes using *OCT4*, *SOX2*, and DAPT, scale bar = 50 μm. **j,** NANOG+/TRA-1-81+ iPSC line generated from human adult keratinocytes using *OCT4*, *SOX2* + DAPT, scale bars = 100 μm. For all experiments, error bars represent the standard deviation between two or three biological replicates and statistical significance was determined using a two-tailed homoscedastic Student's t-test.

Figure 2. γ-secretase inhibition promotes reprogramming by blocking Notch signaling. a, Chemical structure of DBZ. **b,** The efficiency of NANOG+/TRA-1-81+ iPSC generation from human neonatal keratinocytes transduced with *OCT4, KLF4, SOX2*, and *CMYC* and treated with different concentrations of DBZ from days 1-18 post-transduction. **c,** The efficiency of NANOG+/ TRA-1-81+ iPSC generation from human neonatal keratinocytes transduced with *OCT*, *SOX2*, *KLF4*, and *CMYC* and GFP or NOTCH ICD and treated with DMSO or 10 μM DAPT from days 1-18 post-transduction. Cells were transduced with NOTCH ICD or GFP lentivirus 1 day after transduction with the reprogramming factors. **d,** qPCR analysis of expression levels of NOTCH-dependent gene HES1 in human neonatal keratinocytes transduced with dominant-negative MASTERMIND-LIKE-1 (*dnMAML*) or RFP. **e,** The efficiency of NANOG+/TRA-1-81+ iPSC generation from human neonatal keratinocytes transduced with *OCT*, *SOX2*, *KLF4*, and *CMYC* and RFP or *dnMAML* and treated with DMSO or 10 μM DAPT from days 1-18 post-transduction. For all experiments, error bars represent the standard deviation between two or three biological replicates and statistical significance was determined using a two-tailed homoscedastic Student's t-test.

Figure 3. Notch inhibition promotes keratinocyte reprogramming by suppressing p21. a, Schematic of the DAPT treatment time course on human neonatal keratinocytes. **b,** Efficiency of NANOG+/TRA-1-81+ iPSC generation from human neonatal keratinocytes transduced with *OCT4, SOX2, KLF4,* and *CMYC* and treated with intervals of 10 μM DAPT or **c,** 2 μM DBZ. **d,** Western blot for p21 in human neonatal keratinocytes transduced with *OCT4* and *SOX2* and treated with DMSO or 10 μM DAPT. Full blot shown in Supplementary Figure 7c. **e,** Western blot for INVOLUCRIN in human neonatal keratinocytes treated with DMSO, 10 μM DAPT, or 1.2 mM calcium chloride for 6 days. Calcium was used as a positive control to induce keratinocyte differentiation. Full blot shown in Supplementary Figure 7d. **f,** Efficiency of NANOG+/TRA-1-81+ iPSC generation from human neonatal keratinocytes transduced with *OCT4, KLF4, SOX2*, and *CMYC* and a scrambled shRNA or a p21 shRNA at day 0 of reprogramming. DAPT was added at 10 μM. **g,** Efficiency of NANOG+/TRA-1-81+ iPSC generation from human neonatal keratinocytes transduced with *OCT4* and *SOX2* and a scrambled shRNA control or a p21 shRNA at day 0 of reprogramming. DAPT was

added at 2.5 μM. **h,** Efficiency of NANOG+/TRA-1-81+ iPSC generation from human neonatal keratinocytes transduced with *OCT, SOX2, KLF4,* and *CMYC* and GFP or p21 and treated with DMSO or 10 μM DAPT from days 1-18 post-transduction. For all experiments, error bars represent the standard deviation between two-three biological replicates and statistical significance was determined using a two-tailed homoscedastic Student's t-test.

Figure 4. Highly efficient reprogramming with NOTCH and DOT1L inhibition. **a,** Comparison of NANOG+/TRA-1-81+ iPSC generation from *OCT4, SOX2, KLF4,* and *CMYC*-transduced human neonatal keratinocytes using 10 μM DAPT versus other published reprogramming chemicals. "A83" = A8301 (.5 μM), "PD" = PD0325901 (.5 μM), "All from ref (13)" = A8301 (.5 μM), PD0325901 (.5 μM), PS48 (5 μM), sodium butyrate (.25 mM), Parnate (2 μM), CHIR99021 (3 μM), "AZA" = 5-aza-cytidine (.5 μM), "VPA" = valproic acid (.5 mM), "iDOT1L" = EPZ004777 (3 μM). **b,** Comparison of NANOG+/TRA-1-81+ iPSC generation from *OCT4*- and *SOX2*-transduced human neonatal keratinocytes using 2.5 μM DAPT versus other published reprogramming chemicals. **c,** iPSC line generated from human neonatal keratinocytes using *OCT4*, *SOX2*, DAPT, and iDOT1L. scale bars = 100 μm. For all experiments, error bars represent the standard deviation between two-three biological replicates and statistical significance was determined using a two-tailed homoscedastic Student's t-test.

Figure 5. NOTCH inhibition suppresses p21 without reducing p53 activity. **a,** qPCR analysis of p53-dependent genes in human neonatal keratinocytes 3 days after transduction of GFP or *OCT4* and *SOX2*. **b,** Western blot of p53 levels in human neonatal keratinocytes with DMSO or 10 μM DAPT treatment for 3 days. Full blot shown in Supplementary Figure 7g. **c,** qPCR analysis of p53-dependent genes after 10 μM DAPT or 2 μM DBZ treatment for 3 days in *OCT4*, *SOX2*-transduced human keratinocytes. **d,** The efficiency of NANOG+/TRA-1-81+ iPSC generation in *OCT4*, *SOX2*, *KLF4*, and *CMYC*-transduced human neonatal keratinocytes transduced with p53DD or GFP with or without exposure to UV irradiation. **e,** γH2AX immunostaining in human neonatal keratinocytes 10 days after transduction with *OCT4*, *SOX2*, *KLF4*, and *CMYC* and treatment with DAPT, p53DD, or p53 shRNA. Scale bars = 50 μm. **f,** The percentage of TUNEL-positive cells in human neonatal keratinocyte reprogramming cultures with active or inactive p53 (p53DD expression) 10 days after transduction with *OCT4*, *SOX2*, *KLF4*, and *CMYC*. **g,** The number of insertions or deletions (indels) per iPSC line derived under normal, DAPT, or p53DD conditions, as determined by array CGH. For all experiments, error bars represent the standard deviation between two biological replicates and statistical significance was determined using a two-tailed homoscedastic Student's t-test. * denotes significance p-value < .05.

Figure 6. Model of iPSC generation from human keratinocytes. Notch inhibition allows the production of safer oncogene-free iPSCs by suppressing p21 in a p53-independent manner.

Online Methods

iPSC reprogramming experiments

The IACUC committee of Harvard University approved the use of mice for all experiments included in this paper. *Oct4*:GFP neonatal mouse keratinocytes were isolated from P1-P2 pups using an overnight digestion in either .25% trypsin/EDTA or TrypLE (Life Technologies) at 4 degrees Celsius. They were cultured in SFM medium (Life Technologies) on collagen IV-coated plates. Neonatal human epidermal keratinocytes (Lonza) were cultured in Epilife medium (Invitrogen) on collagen-coated plates. Keratinocytes were reprogrammed using retroviruses containing either mouse or human *OCT4, SOX2, KLF4,* and *CMYC* produced in the pMXs backbone. Chemical treatment was initiated 1-2 days after viral transduction and re-administered every other day until the end of the experiment unless otherwise specified. DAPT (EMD Millipore) was used at 10 μM for reprogramming experiments using *OCT4*, *SOX2*, *KLF4*, and *CMYC* and 2.5 μM for *OCT4*, *SOX2* reprogramming experiments unless otherwise noted. DBZ was used at 2 μM. Irradiated mouse embryonic fibroblast feeders were added 6 days after transduction and the media was changed to mouse or human embryonic stem cell medium at that time. Colonies were scored as iPSC colonies if they were *Oct4*::GFP+ in mouse experiments or NANOG+/TRA-1-81+ in human experiments.

Gene expression analysis of iPSCs

Nanostring (Nanostring Technologies) and scorecard analysis was performed as described [34]. iPSCs were cultured in mTesr1 medium (Stem Cell Technologies) prior to RNA isolation. To measure their differentiation propensities, iPSCs were dissociated into

embryoid bodies and cultured in human embryonic stem cell medium without bFGF for 16 days. Cells were then lysed and total RNA was extracted using Trizol (Life Technologies) and purified using the RNeasy kit (QIAGEN). 300 ng to 500 ng of RNA was profiled on the Nano-String nCounter system (Nanostring Technologies) according to manufacturer's instructions. A custom nCounter codeset covering 500 genes that monitor cell state, pluripotency, and differentiation was used [34]. Data analysis was performed with the R statistics package as in [34]. Briefly, the lineage scorecard performs a parametric gene set enrichment analysis on t scores obtained from a pairwise comparison between the cell line of interest and the reference of ES cell-derived EBs.

Differentiation of iPSCs

For teratoma formation, 1-2 million human iPSCs were injected into the kidney capsule of nude mice and harvested 2 months later. Teratomas were sectioned and stained with hematoxylin and eosin for visualization. For the mouse iPSC chimera assay, 10 *Oct4*::GFP+ iPSCs were injected per ICR blastocyst, and 20 blastocysts were transplanted into each pseudopregnant female. Embryos were either allowed to develop to term or harvested at day E12.5 and dissected for genital ridge analysis using a stereomicroscope.

Gene expression analysis of reprogramming cultures

Illumina MouseRef-8 microarrays (Illumina) were used for genome-wide mRNA expression analysis of reprogramming mouse keratinocyte cultures treated with DMSO or 10 μM DAPT. For QPCR analysis, RNA was isolated using Trizol, cDNA synthesis was

performed using the iScript cDNA synthesis kit (Bio-rad), and the SYBR Green qPCR Supermix (Bio-rad) was used for PCR product detection.

Western blots and immunofluorescence

Antibodies detecting mouse Notch (Santa Cruz Biotechnology, sc-6015), human NOTCH (Abcam, ab27526, and Santa Cruz Biotechnology, sc-23307), cleaved human NOTCH (Cell Signaling Technology, 2421), p53 (Santa Cruz Biotechnology, sc-56182), Involucrin (Abcam, Ab53112), and p21 (Cell Signaling Technology 05-345) were used for western blots. Blots were quantified using ImageJ software. Antibodies specific for NANOG (Abcam, AF1997) and TRA-1-81 (Chemicon, MAB4381) were used to identify human iPSCs. A γH2AX (Abcam, ab11175) antibody was used to detect γH2AX foci. Cells in which γH2AX staining covered greater than half the nucleus were scored as positive for γH2AX foci.

UV irradiation assay

UV irradiation was performed at a dosage of 30 J. TUNEL staining was performed using a TUNEL kit (Pharmacia Biosciences).

shRNA/siRNA knockdown experiments

shRNAs and siRNAs were purchased from Sigma and added to reprogramming cultures within 1 day after addition of the reprogramming retroviruses. shRNAs (TRCN0000003753, p53 and TRCN0000287021, p21) were expressed in the pLKO.1

lentiviral backbone. siRNAs were used at 80nM and were transfected into reprogramming cultures using RNAiMAX (Life Technologies).

Array CGH analysis of iPSC lines

Cell Line Genetics performed array CGH analysis of iPSC lines at passage 5 using 4x180K+SNP analysis.

Statistical analysis

For all experiments, error bars represent the standard deviation between two-three biological replicates and statistical significance was determined using a two-tailed homoscedastic Student's t-test.

Accession numbers

Microarray data have been submitted to the GEO repository with accession number GSE35090.

1. Aoi, T. et al. Generation of Pluripotent Stem Cells from Adult Mouse Liver and Stomach Cells. *Science* (2008).
2. Nakagawa, M. et al. Generation of induced pluripotent stem cells without Myc from mouse and human fibroblasts. *Nat Biotechnol* **26**, 101-6 (2008).
3. Kawamura, T. et al. Linking the p53 tumour suppressor pathway to somatic cell reprogramming. *Nature* **460**, 1140-4 (2009).
4. Okita, K. et al. A more efficient method to generate integration-free human iPS cells. *Nat Methods* **8**, 409-12 (2011).
5. Son, M.J. et al. Nicotinamide overcomes pluripotency deficits and reprogramming barriers. *Stem Cells* **31**, 1121-35 (2013).
6. Hong, H. et al. Suppression of induced pluripotent stem cell generation by the p53-p21 pathway. *Nature* **460**, 1132-5 (2009).
7. Utikal, J. et al. Immortalization eliminates a roadblock during cellular reprogramming into iPS cells. *Nature* **460**, 1145-8 (2009).

8. Marion, R.M. et al. A p53-mediated DNA damage response limits reprogramming to ensure iPS cell genomic integrity. *Nature* **460**, 1149-53 (2009).
9. Li, H. et al. The Ink4/Arf locus is a barrier for iPS cell reprogramming. *Nature* **460**, 1136-9 (2009).
10. Li, Y. et al. The p53-PUMA axis suppresses iPSC generation. *Nat Commun* **4**, 2174 (2013).
11. Lake, B.B. et al. Context-dependent enhancement of induced pluripotent stem cell reprogramming by silencing Puma. *Stem Cells* **30**, 888-97 (2012).
12. Guo, S. et al. Nonstochastic reprogramming from a privileged somatic cell state. *Cell* **156**, 649-62 (2014).
13. Lee, Y.L. et al. Sirtuin 1 facilitates generation of induced pluripotent stem cells from mouse embryonic fibroblasts through the miR-34a and p53 pathways. *PLoS One* **7**, e45633 (2012).
14. Brosh, R. et al. p53 counteracts reprogramming by inhibiting mesenchymal-to-epithelial transition. *Cell Death Differ* **20**, 312-20 (2013).
15. Ye, D. et al. MiR-138 promotes induced pluripotent stem cell generation through the regulation of the p53 signaling. *Stem Cells* **30**, 1645-54 (2012).
16. Wang, J. et al. p53-facilitated miR-199a-3p regulates somatic cell reprogramming. *Stem Cells* **30**, 1405-13 (2012).
17. Zhu, S. et al. Reprogramming of human primary somatic cells by OCT4 and chemical compounds. *Cell Stem Cell* **7**, 651-5 (2010).
18. Silva, J. et al. Promotion of reprogramming to ground state pluripotency by signal inhibition. *PLoS Biol* **6**, e253 (2008).
19. Ichida, J.K. et al. A small-molecule inhibitor of tgf-Beta signaling replaces sox2 in reprogramming by inducing nanog. *Cell Stem Cell* **5**, 491-503 (2009).
20. Hou, P. et al. Pluripotent stem cells induced from mouse somatic cells by small-molecule compounds. *Science* **341**, 651-4 (2013).
21. Huangfu, D. et al. Induction of pluripotent stem cells by defined factors is greatly improved by small-molecule compounds. *Nat Biotechnol* **26**, 795-7 (2008).
22. Federation, A.J., Bradner, J.E. & Meissner, A. The use of small molecules in somatic-cell reprogramming. *Trends Cell Biol* **24**, 179-87 (2013).
23. Amabile, G. & Meissner, A. Induced pluripotent stem cells: current progress and potential for regenerative medicine. *Trends Mol Med* **15**, 59-68 (2009).
24. Eminli, S. et al. Differentiation stage determines potential of hematopoietic cells for reprogramming into induced pluripotent stem cells. *Nat Genet* **41**, 968-76 (2009).
25. Gurdon, J.B. The developmental capacity of nuclei taken from intestinal epithelium cells of feeding tadpoles. *J Embryol Exp Morphol* **10**, 622-40 (1962).
26. Li, J., Greco, V., Guasch, G., Fuchs, E. & Mombaerts, P. Mice cloned from skin cells. *Proc Natl Acad Sci U S A* **104**, 2738-43 (2007).
27. Artavanis-Tsakonas, S. & Muskavitch, M.A. Notch: the past, the present, and the future. *Curr Top Dev Biol* **92**, 1-29 (2010).
28. Bray, S.J. Notch signalling: a simple pathway becomes complex. *Nat Rev Mol Cell Biol* **7**, 678-89 (2006).
29. Topley, G.I., Okuyama, R., Gonzales, J.G., Conti, C. & Dotto, G.P. p21(WAF1/Cip1) functions as a suppressor of malignant skin tumor formation

and a determinant of keratinocyte stem-cell potential. *Proc Natl Acad Sci U S A* **96**, 9089-94 (1999).
30. Missero, C., Di Cunto, F., Kiyokawa, H., Koff, A. & Dotto, G.P. The absence of p21Cip1/WAF1 alters keratinocyte growth and differentiation and promotes ras-tumor progression. *Genes Dev* **10**, 3065-75 (1996).
31. Aasen, T. & Belmonte, J.C. Isolation and cultivation of human keratinocytes from skin or plucked hair for the generation of induced pluripotent stem cells. *Nat Protoc* **5**, 371-82 (2010).
32. Aasen, T. et al. Efficient and rapid generation of induced pluripotent stem cells from human keratinocytes. *Nat Biotechnol* **26**, 1276-84 (2008).
33. Blanpain, C., Lowry, W.E., Pasolli, H.A. & Fuchs, E. Canonical notch signaling functions as a commitment switch in the epidermal lineage. *Genes Dev* **20**, 3022-35 (2006).
34. Bock, C. et al. Reference Maps of Human ES and iPS Cell Variation Enable High-Throughput Characterization of Pluripotent Cell Lines. *Cell* **144**, 439-52 (2011).
35. Fuwa, H. et al. Divergent synthesis of multifunctional molecular probes to elucidate the enzyme specificity of dipeptidic gamma-secretase inhibitors. *ACS Chem Biol* **2**, 408-18 (2007).
36. Nam, Y., Sliz, P., Song, L., Aster, J.C. & Blacklow, S.C. Structural basis for cooperativity in recruitment of MAML coactivators to Notch transcription complexes. *Cell* **124**, 973-83 (2006).
37. Nam, Y., Weng, A.P., Aster, J.C. & Blacklow, S.C. Structural requirements for assembly of the CSL.intracellular Notch1.Mastermind-like 1 transcriptional activation complex. *J Biol Chem* **278**, 21232-9 (2003).
38. Lefort, K. & Dotto, G.P. Notch signaling in the integrated control of keratinocyte growth/differentiation and tumor suppression. *Semin Cancer Biol* **14**, 374-86 (2004).
39. Jones, P.H. & Watt, F.M. Separation of human epidermal stem cells from transit amplifying cells on the basis of differences in integrin function and expression. *Cell* **73**, 713-24 (1993).
40. Kavian, N. et al. Targeting ADAM-17/notch signaling abrogates the development of systemic sclerosis in a murine model. *Arthritis Rheum* **62**, 3477-87.
41. Allen, A.S. et al. De novo mutations in epileptic encephalopathies. *Nature* **501**, 217-21.
42. Huangfu, D. et al. Induction of pluripotent stem cells from primary human fibroblasts with only Oct4 and Sox2. *Nat Biotechnol* (2008).
43. Mikkelsen, T.S. et al. Dissecting direct reprogramming through integrative genomic analysis. *Nature* **454**, 49-55 (2008).
44. Onder, T.T. et al. Chromatin-modifying enzymes as modulators of reprogramming. *Nature* **483**, 598-602 (2012).
45. Gore, A. et al. Somatic coding mutations in human induced pluripotent stem cells. *Nature* **471**, 63-7 (2011).

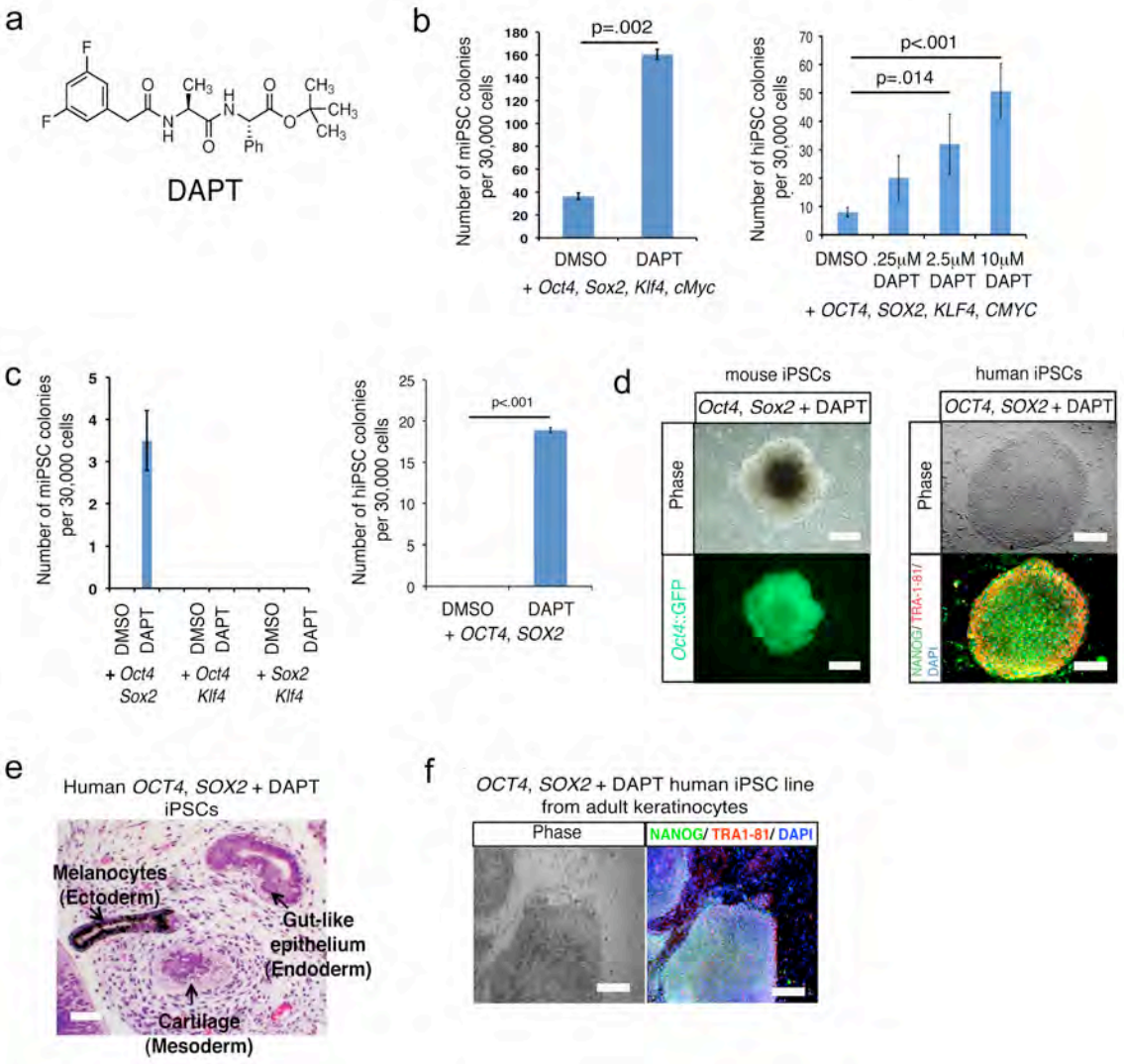
a
DAPT
b
Number of miPSC colonies per 30,000 cells
p=.002
DMSO
DAPT
+ Oct4, Sox2, Klf4, cMyc
Number of hiPSC colonies per 30,000 cells
p<.001
p=.014
DMSO
.25μM DAPT
2.5μM DAPT
10μM DAPT
+ OCT4, SOX2, KLF4, CMYC
c
Number of miPSC colonies per 30,000 cells
DMSO
DAPT
+ Oct4 Sox2
+ Oct4 Klf4
+ Sox2 Klf4
Number of hiPSC colonies per 30,000 cells
p<.001
DMSO
DAPT
+ OCT4, SOX2
d
mouse iPSCs
Oct4, Sox2 + DAPT
Phase
Oct4::GFP
human iPSCs
OCT4, SOX2 + DAPT
Phase
NANOG/ TRA-1-81/ DAPI
e
Human OCT4, SOX2 + DAPT iPSCs
Melanocytes (Ectoderm)
Gut-like epithelium (Endoderm)
Cartilage (Mesoderm)
f
OCT4, SOX2 + DAPT human iPSC line from adult keratinocytes
Phase
NANOG/ TRA1-81/ DAPI

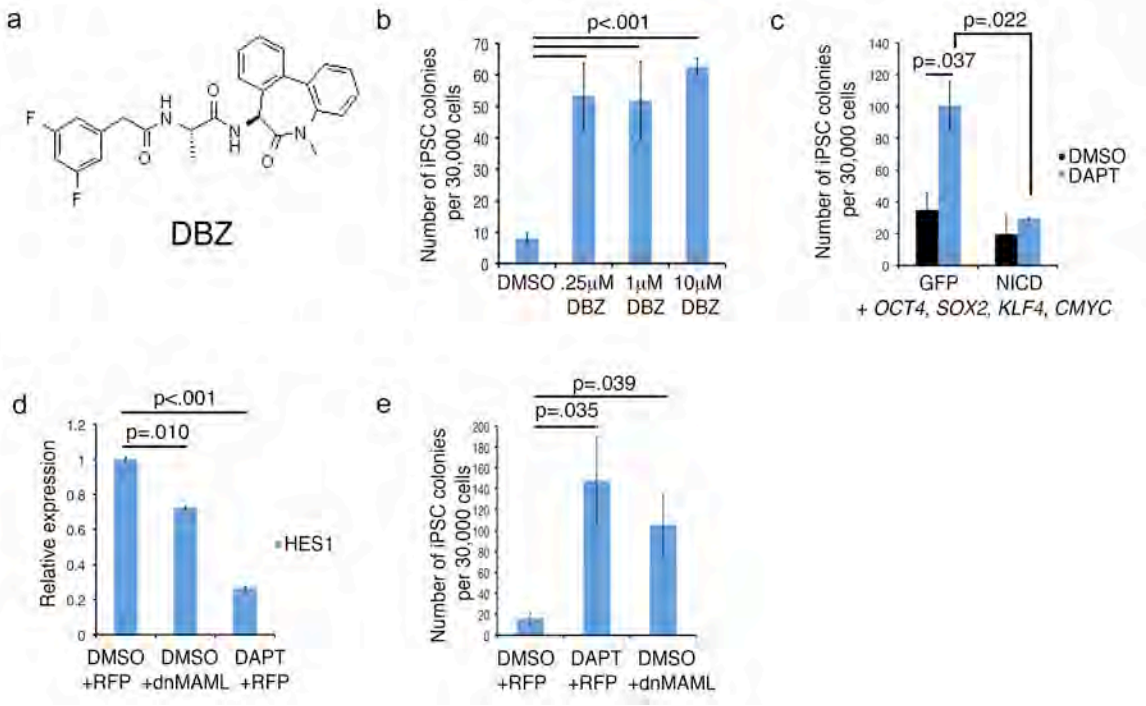
a
DBZ
b
p<.001
Number of iPSC colonies per 30,000 cells
DMSO
.25μM DBZ
1μM DBZ
10μM DBZ
c
p=.022
p=.037
Number of iPSC colonies per 30,000 cells
DMSO
DAPT
GFP
NICD
+ OCT4, SOX2, KLF4, CMYC
d
p<.001
p=.010
Relative expression
HES1
DMSO +RFP
DMSO +dnMAML
DAPT +RFP
e
p=.039
p=.035
Number of iPSC colonies per 30,000 cells
DMSO +RFP
DAPT +RFP
DMSO +dnMAML

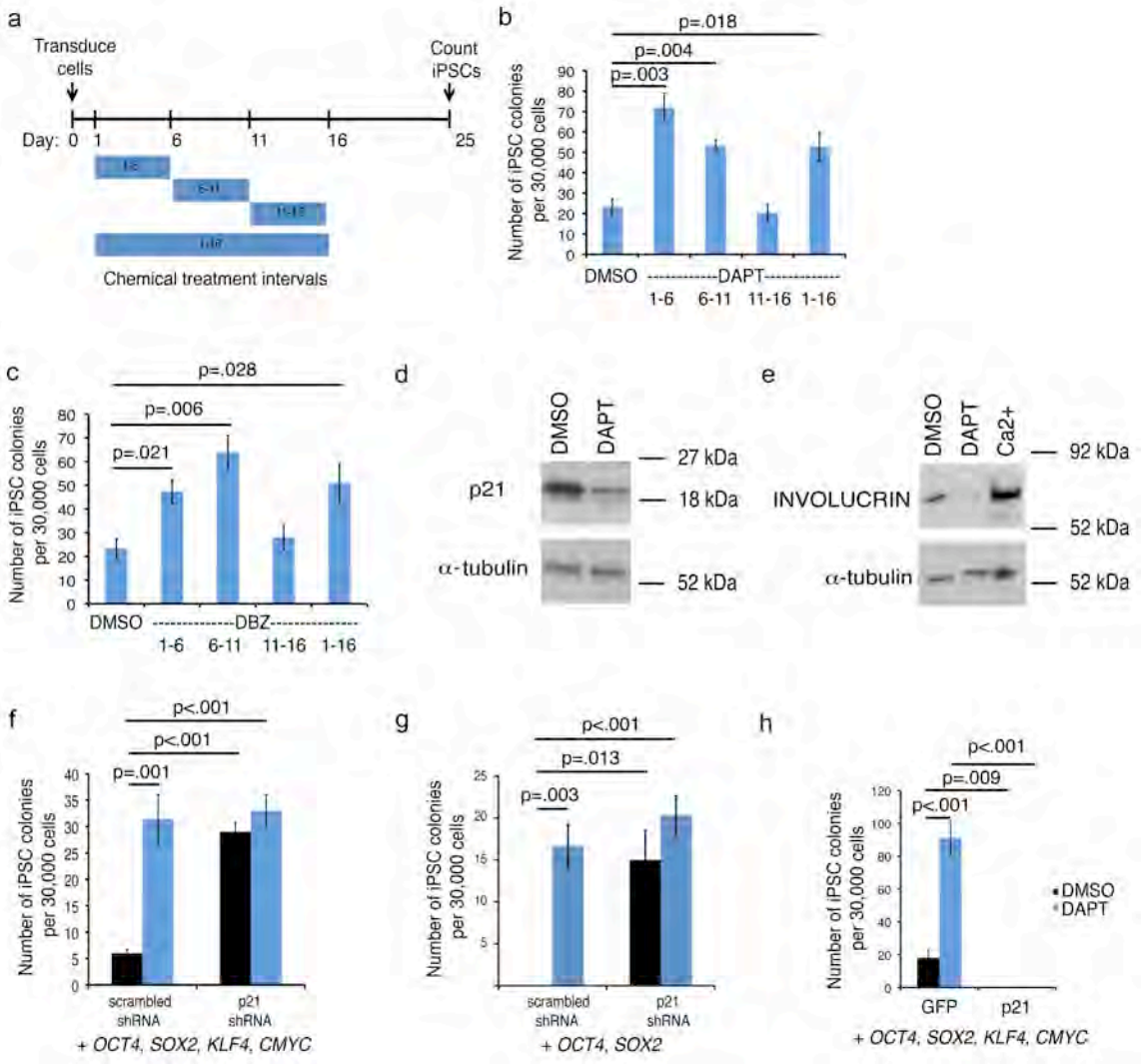
a
Transduce cells
Count iPSCs
Day: 0 1 6 11 16 25
Chemical treatment intervals
b
p=.018
p=.004
p=.003
Number of iPSC colonies per 30,000 cells
DMSO
DAPT
1-6 6-11 11-16 1-16
c
p=.028
p=.006
p=.021
Number of iPSC colonies per 30,000 cells
DMSO
DBZ
1-6 6-11 11-16 1-16
d
DMSO
DAPT
p21
27 kDa
18 kDa
α-tubulin
52 kDa
e
DMSO
DAPT
Ca2+
INVOLUCRIN
92 kDa
52 kDa
α-tubulin
52 kDa
f
p<.001
p<.001
p=.001
Number of iPSC colonies per 30,000 cells
scrambled shRNA
p21 shRNA
+ OCT4, SOX2, KLF4, CMYC
g
p<.001
p=.013
p=.003
Number of iPSC colonies per 30,000 cells
scrambled shRNA
p21 shRNA
+ OCT4, SOX2
h
p<.001
p=.009
p<.001
Number of iPSC colonies per 30,000 cells
DMSO
DAPT
GFP
p21
+ OCT4, SOX2, KLF4, CMYC

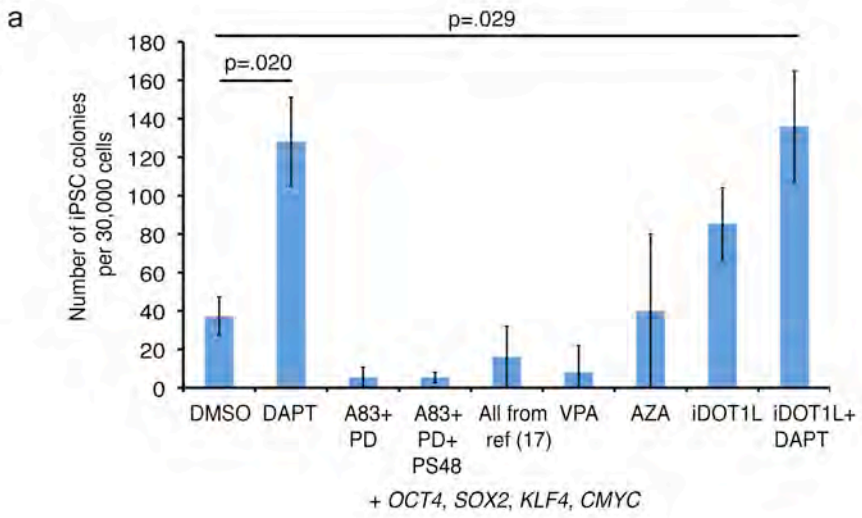
a
p=.029
p=.020
Number of iPSC colonies per 30,000 cells
180
160
140
120
100
80
60
40
20
0
DMSO
DAPT
A83+ PD
A83+ PD+ PS48
All from ref (17)
VPA
AZA
iDOT1L
iDOT1L+ DAPT
+ OCT4, SOX2, KLF4, CMYC

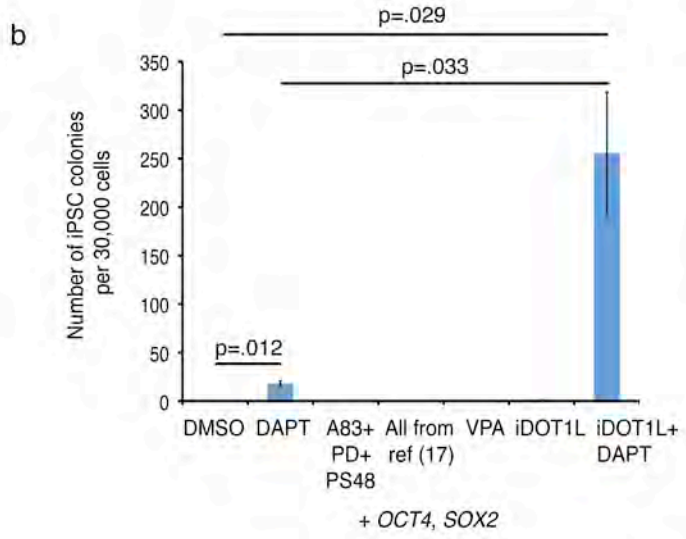
b
p=.029
p=.033
Number of iPSC colonies per 30,000 cells
350
300
250
200
150
100
50
0
p=.012
DMSO
DAPT
A83+ PD+ PS48
All from ref (17)
VPA
iDOT1L
iDOT1L+ DAPT
+ OCT4, SOX2

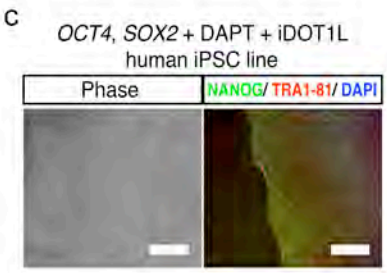
c
OCT4, SOX2 + DAPT + iDOT1L
human iPSC line
Phase
NANOG/ TRA1-81/ DAPI

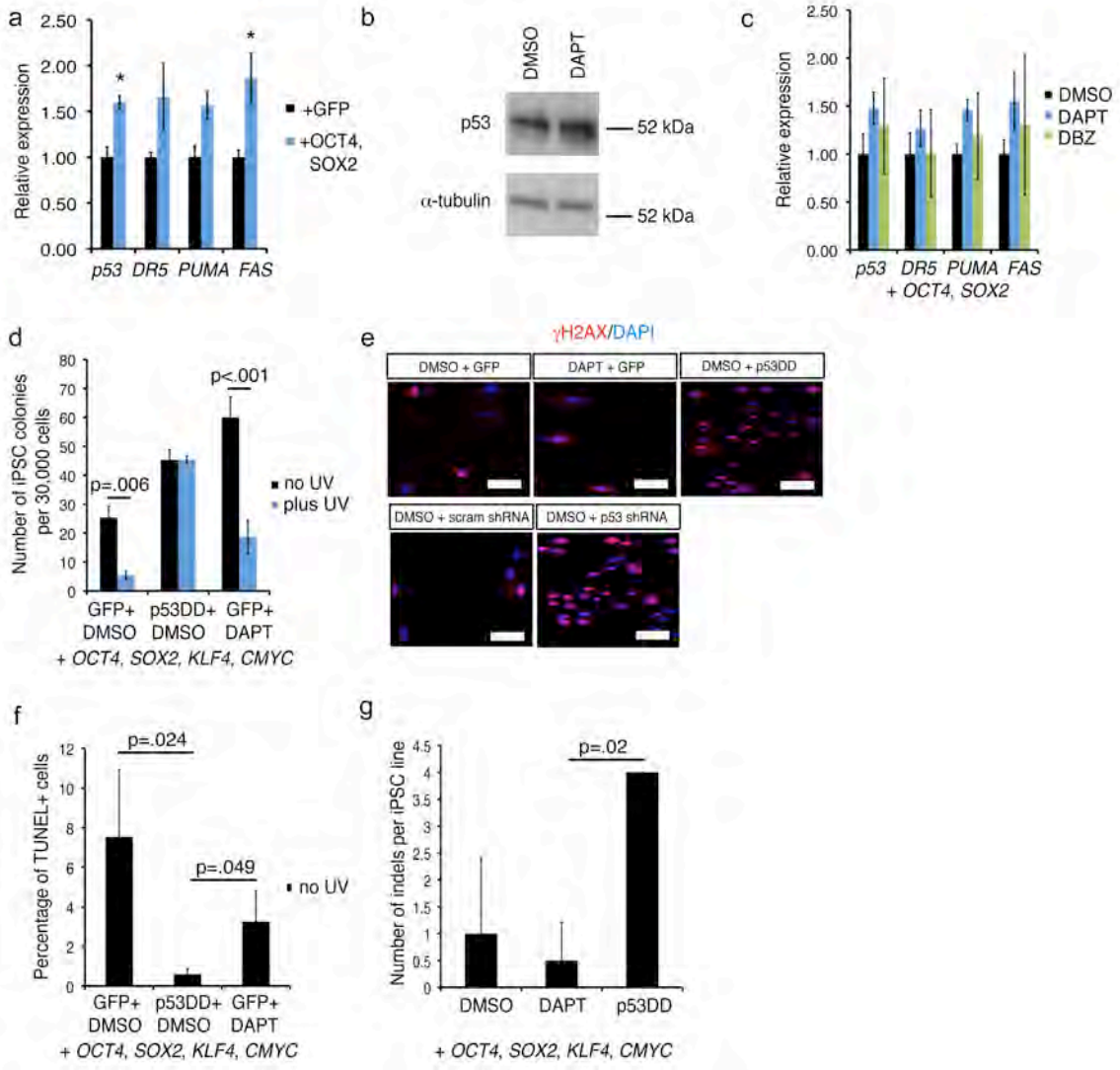
a
Relative expression
2.50
2.00
1.50
1.00
0.50
0.00
*
*
+GFP
+OCT4, SOX2
p53 DR5 PUMA FAS
b
DMSO
DAPT
p53
52 kDa
α-tubulin
52 kDa
c
Relative expression
DMSO
DAPT
DBZ
p53 DR5 PUMA FAS
+ OCT4, SOX2
d
Number of iPSC colonies per 30,000 cells
p=.006
p<.001
no UV
plus UV
GFP+ DMSO
p53DD+ DMSO
GFP+ DAPT
+ OCT4, SOX2, KLF4, CMYC
e
γH2AX/DAPI
DMSO + GFP
DAPT + GFP
DMSO + p53DD
DMSO + scram shRNA
DMSO + p53 shRNA
f
Percentage of TUNEL+ cells
p=.024
p=.049
no UV
GFP+ DMSO
p53DD+ DMSO
GFP+ DAPT
+ OCT4, SOX2, KLF4, CMYC
g
Number of indels per iPSC line
p=.02
DMSO
DAPT
p53DD
+ OCT4, SOX2, KLF4, CMYC

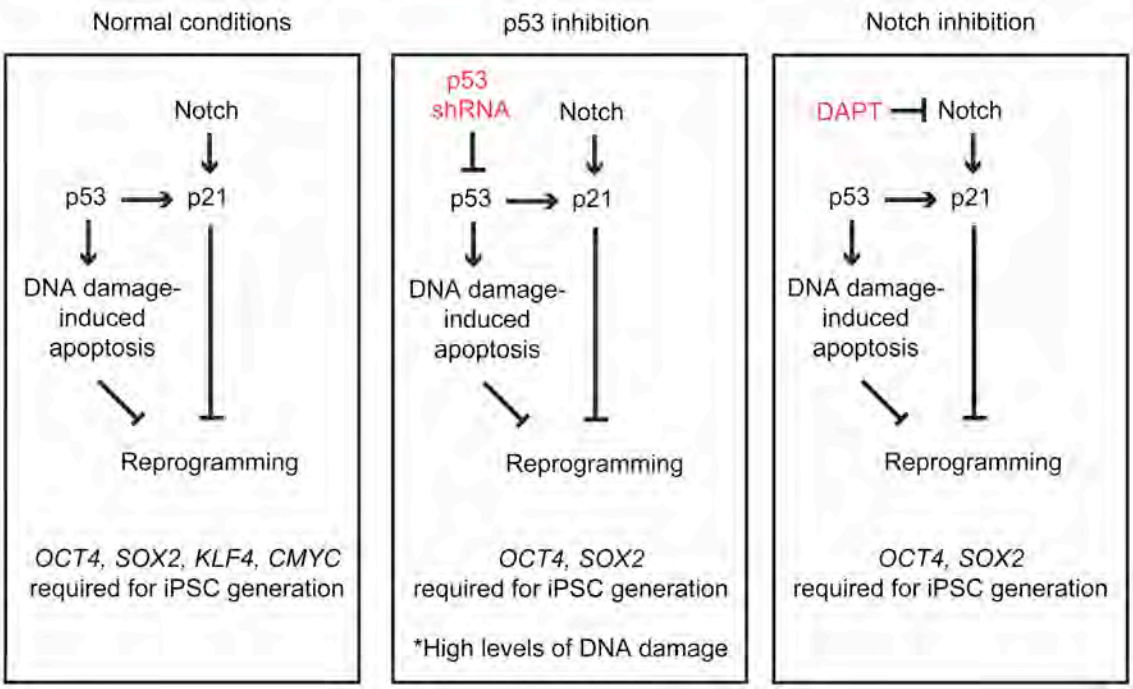
Normal conditions
Notch
p53
p21
DNA damage-induced apoptosis
Reprogramming
OCT4, SOX2, KLF4, CMYC required for iPSC generation
p53 inhibition
p53 shRNA
Notch
p53
p21
DNA damage-induced apoptosis
Reprogramming
OCT4, SOX2 required for iPSC generation
*High levels of DNA damage
Notch inhibition
DAPT
Notch
p53
p21
DNA damage-induced apoptosis
Reprogramming
OCT4, SOX2 required for iPSC generation

Supplementary Information

Notch inhibition allows oncogene independent generation of iPS cells

Justin K. Ichida*, Julia TCW*, Luis A. Williams, Ava C. Carter, Yingxiao Shi, Marcelo T. Moura, Michael Ziller, Sean Singh, Giovanni Amabile, Christoph Bock, Akihiro Umezawa, Lee L. Rubin, James E. Bradner, Hidenori Akutsu, Alexander Meissner, Kevin Eggan

Supplementary Results

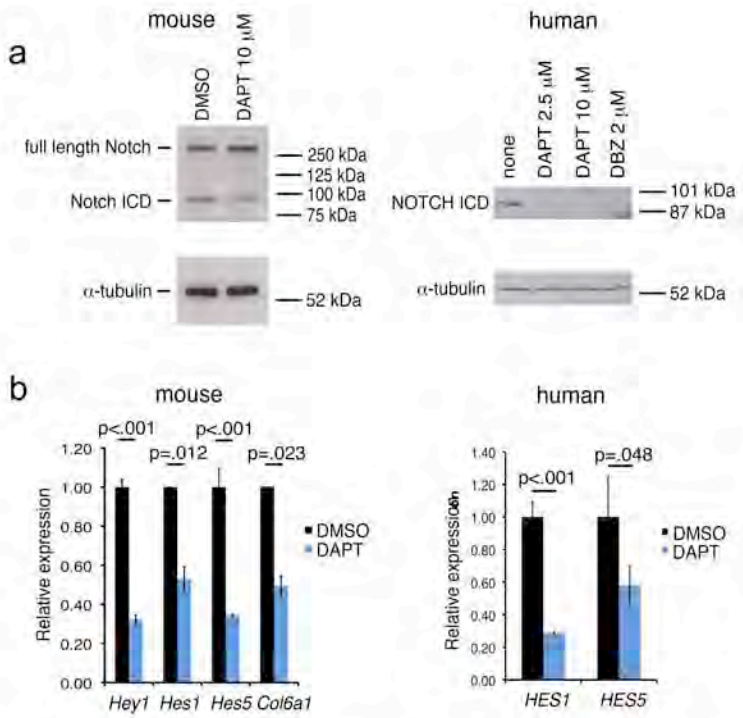

Supplementary figure 1. DAPT treatment inhibits Notch signaling in mouse and human keratinocytes.
a, Western blot for Notch1 on *OCT4, SOX2, KLF4,* and *CMYC*-transduced mouse and human keratinocytes with or without DAPT or DBZ treatment for 3 days. Notch ICD - Notch intracellular domain. Full blots shown in Supplementary Figures 7 a,b. **b,** qPCR analysis for the expression of Notch-dependent genes in mouse and human keratinocytes transduced with the reprogramming factors +/- 10 μM DAPT treatment for 3 days. For all experiments, error bars represent the standard deviation between two or three biological replicates and statistical significance was determined using a two-tailed homoscedastic Student's t-test.

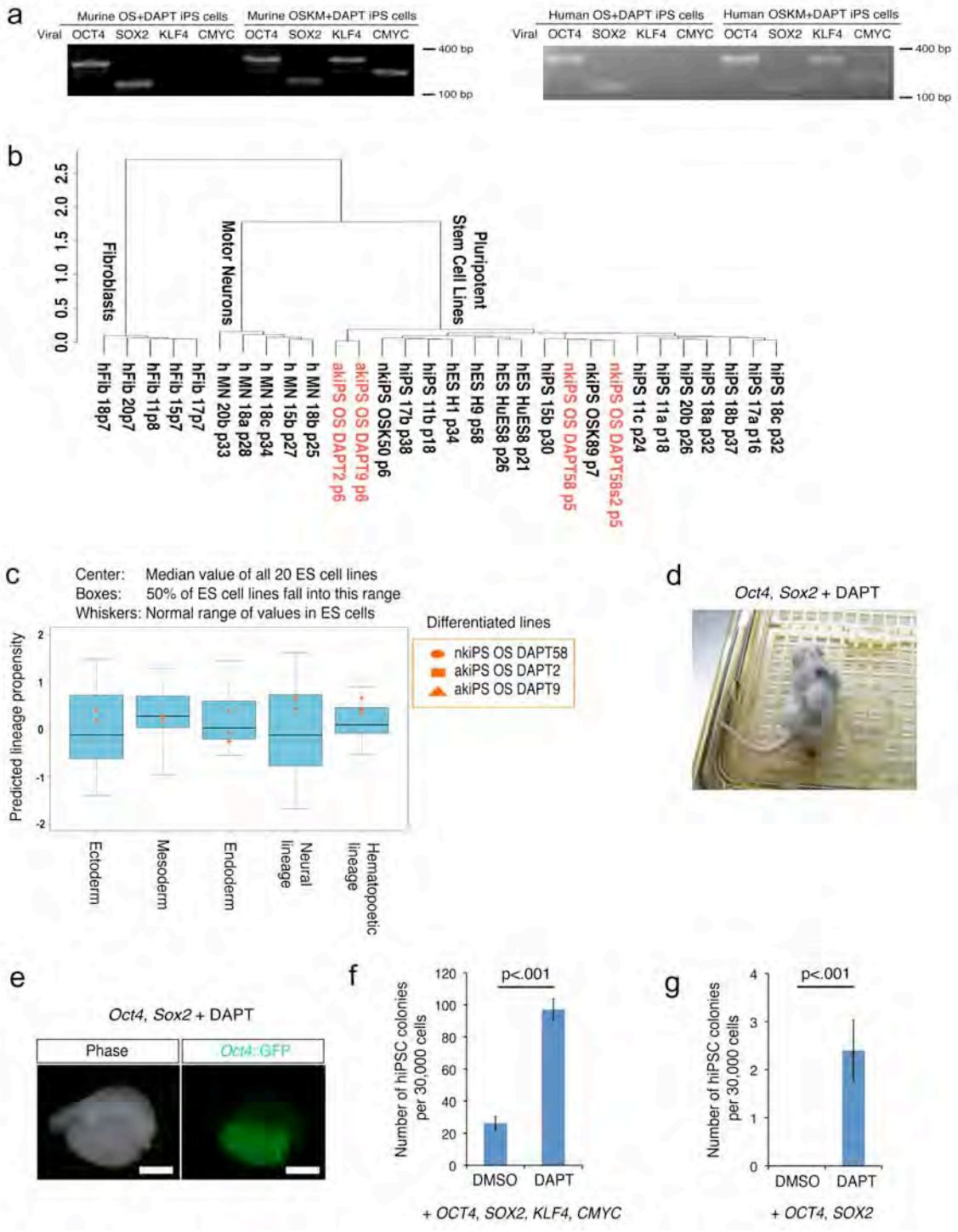
a
Murine OS+DAPT iPS cells
Murine OSKM+DAPT iPS cells
Viral OCT4 SOX2 KLF4 CMYC OCT4 SOX2 KLF4 CMYC
400 bp
100 bp
Human OS+DAPT iPS cells
Human OSKM+DAPT iPS cells
Viral OCT4 SOX2 KLF4 CMYC OCT4 SOX2 KLF4 CMYC
400 bp
100 bp
b
Predicted lineage propensity
0.0 0.5 1.0 1.5 2.0 2.5
Fibroblasts
Motor Neurons
Pluripotent Stem Cell Lines
hFib 18p7
hFib 20p7
hFib 11p8
hFib 15p7
hFib 17p7
h MN 20b p33
h MN 18a p28
h MN 18c p34
h MN 15b p27
h MN 18b p25
akiPS OS DAPT2 p6
akiPS OS DAPT9 p6
nkiPS OSK50 p6
hiPS 17b p38
hiPS 11b p18
hES H1 p34
hES H9 p58
hES HuES8 p26
hES HuES8 p21
hiPS 15b p30
nkiPS OS DAPT58 p5
nkiPS OSK89 p7
nkiPS OS DAPT58s2 p5
hiPS 11c p24
hiPS 11a p18
hiPS 20b p26
hiPS 18a p32
hiPS 18b p37
hiPS 17a p16
hiPS 18c p32
c
Center: Median value of all 20 ES cell lines
Boxes: 50% of ES cell lines fall into this range
Whiskers: Normal range of values in ES cells
Predicted lineage propensity
2
1
0
-1
-2
Differentiated lines
nkiPS OS DAPT58
akiPS OS DAPT2
akiPS OS DAPT9
Ectoderm
Mesoderm
Endoderm
Neural lineage
Hematopoetic lineage
d
Oct4, Sox2 + DAPT
e
Oct4, Sox2 + DAPT
Phase
Oct4::GFP
f
Number of hiPSC colonies per 30,000 cells
120
100
80
60
40
20
0
p<.001
DMSO DAPT
+ OCT4, SOX2, KLF4, CMYC
g
Number of hiPSC colonies per 30,000 cells
4
3
2
1
0
p<.001
DMSO DAPT
+ OCT4, SOX2

Supplementary figure 2. DAPT treatment promotes mouse and human keratinocyte reprogramming. a, PCR genotyping of transgenic insertions in genomic DNA from DAPT iPSCs. **b,** Hierarchical clustering of mRNA expression profiles of pluripotent stem cell lines. "hES" = ESCs, "hiPS" = fibroblast-derived iPSCs, "nkiPSOSK50" = keratinocyte-derived iPSC lines induced with OCT4, SOX2, and KLF4, "hFib" = primary fibroblast lines, "hMN" = hESC-derived motor neurons, "nkiPS OSDAPT58" = human iPSC line generated from neonatal keratinocytes with OCT4, SOX2, and DAPT, "nkiPS OSDAPT58s2" = a subclone from passage 2 of nkiPS OSDAPT58, "akiPS OSDAPT2" and "akiPSOSDAPT9" = two independent iPSC lines derived from adult keratinocytes using OCT4, SOX2, and DAPT. **c,** Lineage scorecard analysis of embryoid bodies differentiated for 16 days, showing the propensities with which the DAPT-iPSCs differentiate into endodermal, mesodermal, and ectodermal lineages. **d,** Chimeric mouse generated from C57Bl/6 *OCT4*, *SOX2* + DAPT mouse iPSCs injected into ICR (albino) blastocysts. **e,** The E13.5 genital ridge of an embryo derived from non-transgenic blastocysts injected with *OCT4*, *SOX2* + DAPT mouse iPSCs derived from *Oct4*::GFP keratinocytes. Scale bars = 400 μm. **f,** Efficiency of iPSC generation from human adult keratinocytes transduced with *OCT4, KLF4, SOX2*, and *CMYC*, treated with or without 10 μM DAPT. **g,** Efficiency of iPSC generation from human adult keratinocytes transduced with *OCT4* and *SOX2,* treated with or without 2.5 μM DAPT. For all experiments, error bars represent the standard deviation between two or three biological replicates and statistical significance was determined using a two-tailed homoscedastic Student's t-test.

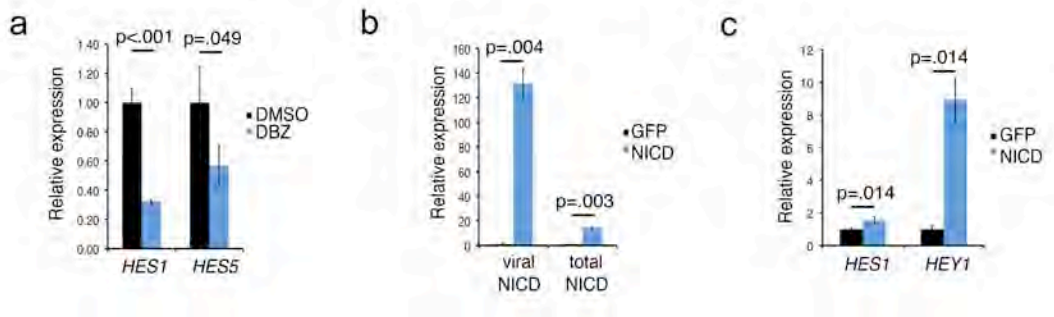

Supplementary figure 3. γ-secretase inhibition promotes reprogramming by blocking Notch signaling. a, qPCR analysis for mRNA levels of NOTCH-dependent genes in human keratinocytes transduced with the reprogramming factors with or without 2 μM DBZ treatment for 3 days. **b,** qPCR analysis for viral NOTCH intracellular domain (NICD) and total NOTCH ICD in human neonatal keratinocytes transduced with lentivirus encoding NOTCH ICD or GFP. **c,** qPCR analysis of expression levels of NOTCH-dependent genes in human neonatal keratinocytes transduced with Notch ICD or GFP. For all experiments, error bars represent the standard deviation between two or three biological replicates and statistical significance was determined using a two-tailed homoscedastic Student's t-test.

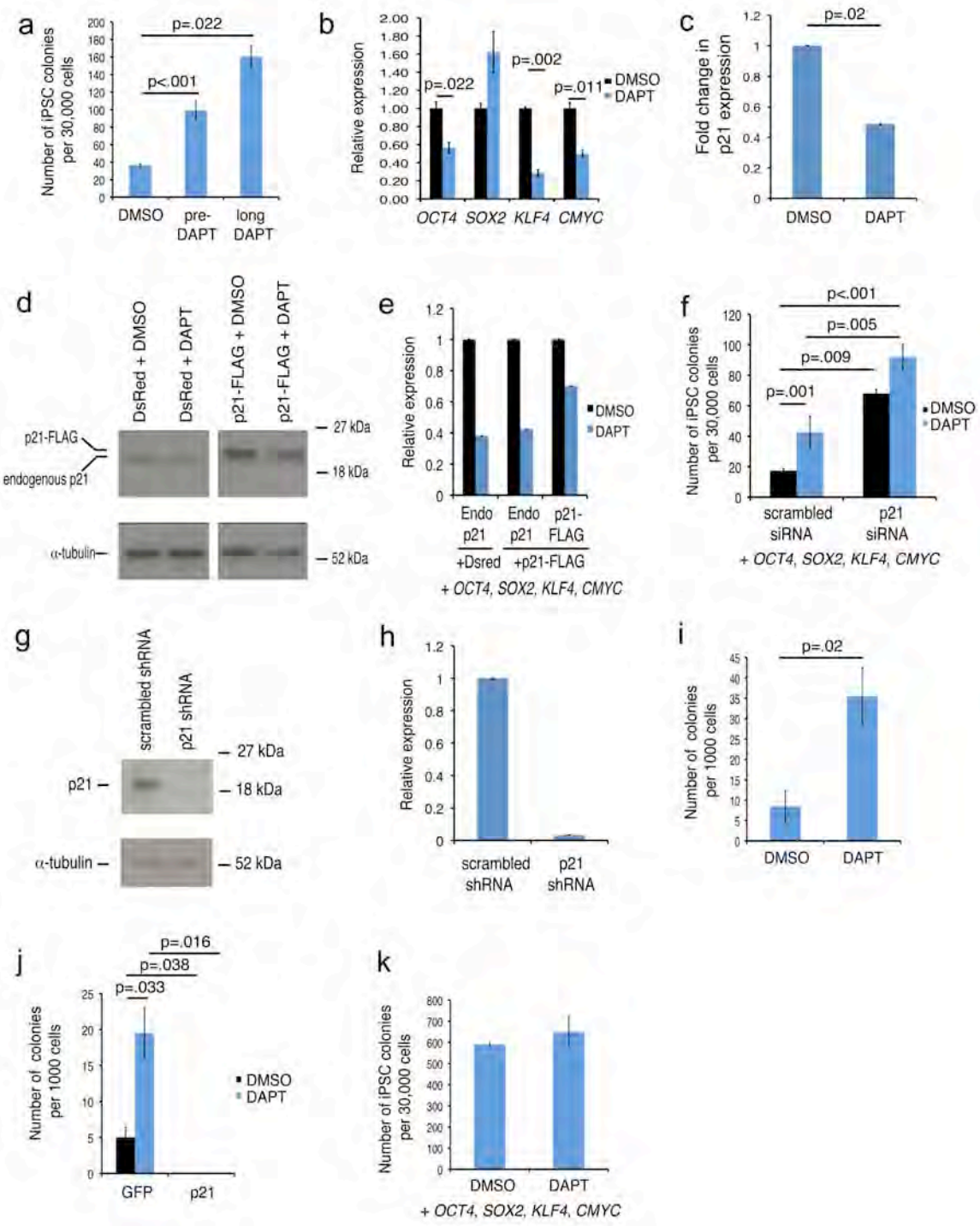
a
Number of iPSC colonies per 30,000 cells
p=.022
p<.001
DMSO
pre-DAPT
long DAPT
b
Relative expression
p=.022
p=.002
p=.011
DMSO
DAPT
OCT4 SOX2 KLF4 CMYC
c
Fold change in p21 expression
p=.02
DMSO
DAPT
d
DsRed + DMSO
DsRed + DAPT
p21-FLAG + DMSO
p21-FLAG + DAPT
p21-FLAG
endogenous p21
27 kDa
18 kDa
α-tubulin
52 kDa
e
Relative expression
DMSO
DAPT
Endo p21
Endo p21
p21-FLAG
+Dsred
+p21-FLAG
+ OCT4, SOX2, KLF4, CMYC
f
Number of iPSC colonies per 30,000 cells
p<.001
p=.005
p=.009
p=.001
DMSO
DAPT
scrambled siRNA
p21 siRNA
+ OCT4, SOX2, KLF4, CMYC
g
scrambled shRNA
p21 shRNA
p21
27 kDa
18 kDa
α-tubulin
52 kDa
h
Relative expression
scrambled shRNA
p21 shRNA
i
Number of colonies per 1000 cells
p=.02
DMSO
DAPT
j
Number of colonies per 1000 cells
p=.016
p=.038
p=.033
DMSO
DAPT
GFP
p21
k
Number of iPSC colonies per 30,000 cells
DMSO
DAPT
+ OCT4, SOX2, KLF4, CMYC

Supplementary figure 4. Notch inhibition promotes keratinocyte reprogramming by suppressing p21. a, Reprogramming efficiency over a time course of 10 μM DAPT treatment in mouse keratinocytes transduced with *OCT4, SOX2, KLF4,* and *CMYC*. "pre-DAPT" = treatment from 6 days before transduction-1 day before transduction, "long DAPT" = treatment from 6 days before transduction-18 days post-transduction. **b,** qPCR analysis of endogenous pluripotency genes in human keratinocytes treated with DMSO or 10 μM DAPT. **c,** qPCR analysis of p21 expression in human neonatal keratinocytes transduced with *OCT4*, *SOX2* and treated with DMSO or 10 μM DAPT. **d,** Western blot using a p21-specific antibody detecting endogenous p21 and the p21-FLAG-tagged protein. Full blot in Supplementary Figure 7e. **e,** Quantification of p21 western blot. **f,** Reprogramming efficiency of mouse keratinocytes transduced with *OCT4, KLF4, SOX2,* and *CMYC* and treated with 80 nM scrambled or p21 siRNA at day 0. **g,** p21 western blot in human neonatal keratinocytes transduced with the reprogramming factors and a scrambled or p21 shRNA. Full blot in Supplementary Figure 7f. **h,** Quantification of p21 western blot. **i,** Colony forming assay on human neonatal keratinocytes. Colonies >35 cells were scored positive. **j,** Colony forming assay using human neonatal keratinocytes transduced with GFP or p21. **k,** Reprogramming efficiency of MEFs transduced with *OCT4, SOX2, KLF4,* and *CMYC* and treated with DMSO or 10 μM DAPT. For all experiments, error bars represent the standard deviation between two or three biological replicates and statistical significance was determined using a two-tailed homoscedastic Student's t-test.

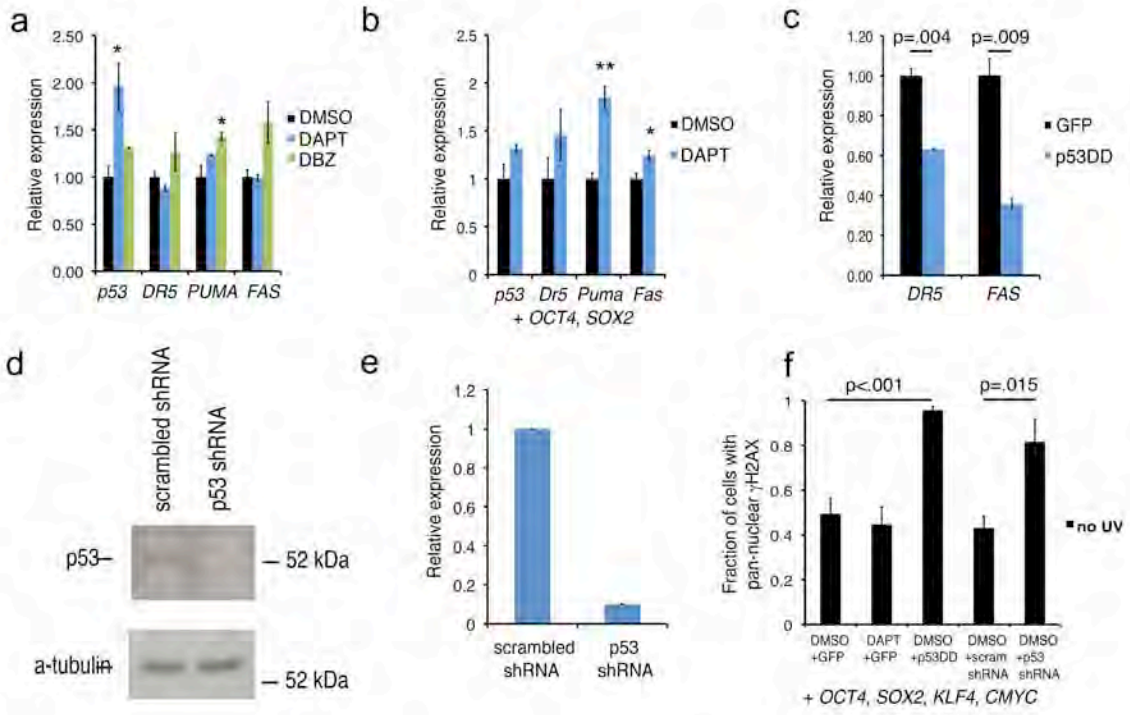

Supplementary figure 5. Notch inhibition suppresses p21 without reducing p53 activity. a, qPCR analysis of p53-dependent genes after 10 μM DAPT or 2 μM DBZ treatment for 3 days in untransduced human neonatal keratinocytes. **b,** qPCR analysis of p53-dependent genes after 10 μM DAPT treatment for 3 days in *OCT4, SOX2*-transduced mouse neonatal keratinocytes. **c,** qPCR analysis of p53-dependent genes in human neonatal keratinocytes with GFP or p53DD overexpression for 3 days. **d,** Western blot using a p53-specific antibody on human neonatal keratinocytes transduced with the reprogramming factors and either a scrambled or p53 shRNA. Full blot shown in Supplementary Figure 7h. **e,** Quantification of the western blot for endogenous p53 levels. **f,** Quantification of pan-nuclear γH2AX immunostaining in human neonatal keratinocytes 10 days after transduction with *OCT4, SOX2, KLF4,* and *CMYC* and treatment with DAPT, p53DD, or p53 shRNA. For all experiments, error bars represent the standard deviation between two biological replicates and statistical significance was determined using a two-tailed homoscedastic Student's t-test. * denotes significance p-value < .05. ** denotes significance p-value < .01.

Amp = amplification
Del = deletion

KSOM + DMSO iPSC line #1: Total Amp/Del: 0

KSOM + DMSO iPSC line # 2: Total Amp/Del: 2

Chr	Start-Stop(bp)	Size(bp)	Cytoband	#Probes	Amp/Del	Annotations
chr5	146254310-147372489	1,118,180	q32	57	0.283914	PPP2R2B, STK32A, DPYSL3, JAKMIP2, SPINK1, SCGB3A2, C5orf46
chr14	19467177-20421677	954,501	q11.2	10	-0.618286	POTEG, POTEM, OR11H2, OR4Q3, OR4M1, OR4N2, OR4K2, OR4K5, OR4K1

KSOM + DAPT iPSC line #1: Total Amp/Del: 0

KSOM + DAPT iPSC line #2: Total Amp/Del: 1

Chr	Start-Stop(bp)	Size(bp)	Cytoband	#Probes	Amp/Del	Annotations
chr14	19467177-20421677	954,501	q11.2	10	-0.517746	POTEG, POTEM, OR11H2, OR4Q3, OR4M1, OR4N2, OR4K2, OR4K5, OR4K1

KSOM + p53DD iPSC line #1: Total Amp/Del: 4

Chr	Start-Stop(bp)	Size(bp)	Cytoband	#Probes	Amp/Del	Annotations
chr6	123590947-124302546	711,600	q22.31	26	0.616509	TRDN, NKAIN2
chr14	61081192-61116160	34,969	q23.1	21	0.389851	SIX1
chr20	57459300-57468102	8,803	q13.32	16	0.636485	GNAS
chr22	19746363-19749476	3,114	q11.21	8	0.819500	TBX1

KSOM + p53DD iPSC line #2: Total Amp/Del: 4

Chr	Start-Stop(bp)	Size(bp)	Cytoband	#Probes	Amp/Del	Annotations
chr3	60776287-61125206	348,920	p14.2	12	-0.877286	FHIT
chr14	19467177-20421677	954,501	q11.2	10	-0.483897	POTEG, POTEM, OR11H2, OR4Q3, OR4M1, OR4N2, OR4K2, OR4K5, OR4K1
chr15	92716928-102399819	9,682,892	q26.1 - q26.3	478	-0.787881	ST8SIA2, C15orf32, LOC100144604, FAM174B, ASB9P1, LOC100507217, CHD2, MIR3175, RGMA, MCTP2, LOC400456, LOC145820, NR2F2, MIR1469, SPATA8, LOC91948, ARRDC4, FAM169B, IGF1R, PGPEP1L, SYNM, TTC23, LRRC28, MEF2A, LYSMD4...
chr20	57463534-57464587	1,054	q13.32	7	0.541517	GNAS

Supplementary Figure 6. Array CGH analysis of iPSC lines generated from keratinocytes with reprogramming factors alone, with DAPT, or with p53DD. Human neonatal keratinocytes were transduced with *OCT4, SOX2, KLF4*, and *CMYC* either alone, with p53DD, or with DAPT treatment. Two resulting iPSC lines from each condition were subjected to 4x180K+SNP array CGH analysis at passage 5.

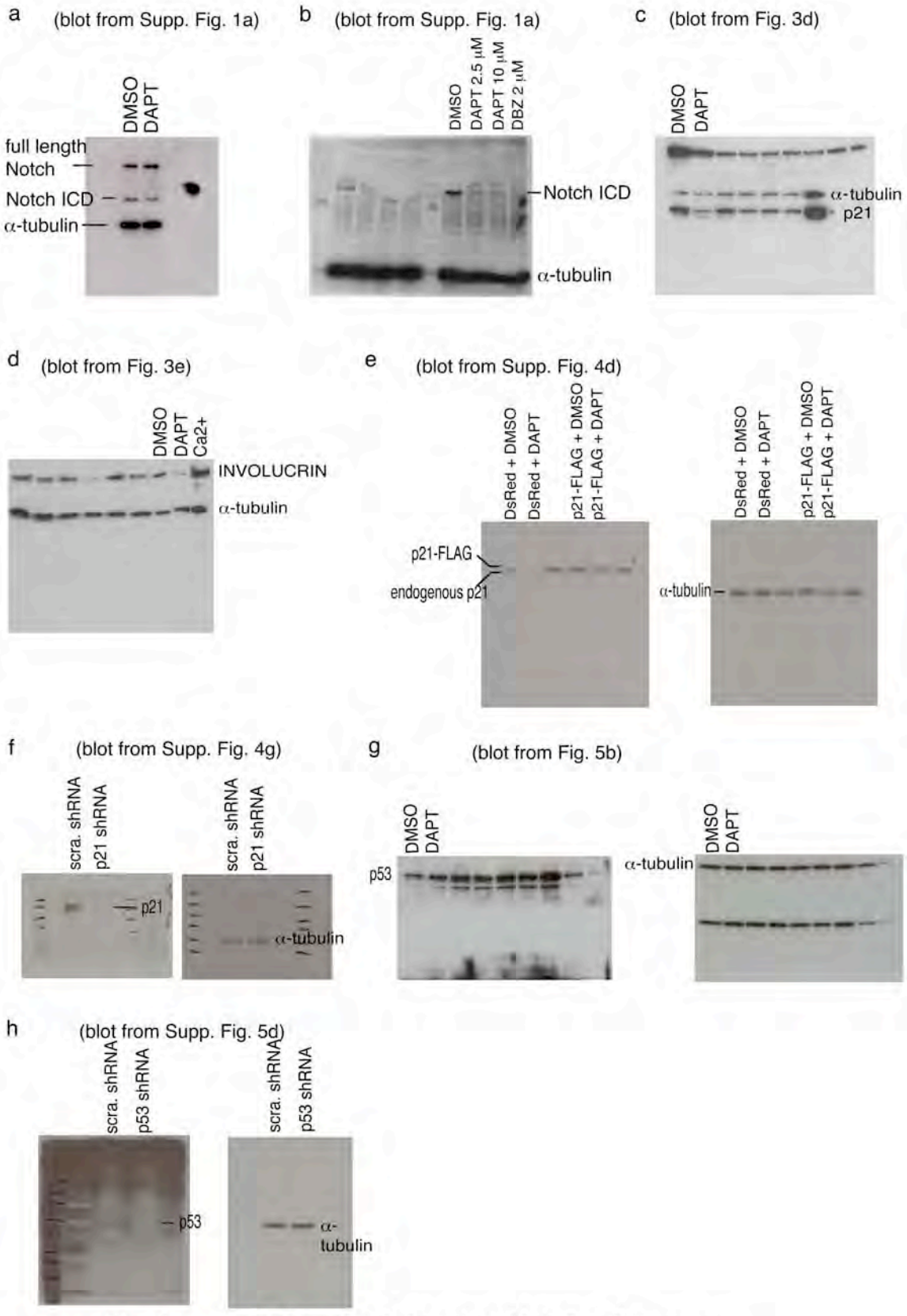

Supplementary Figure 7. Full western blots for all figures.